Journal of Automation, Electronics and Electrical Engineering

DETERMINATION OF THE CURRENT-VOLTAGE CHARACTERISTICS OF THE PHOTOVOLTAIC CELLS USING THE COACHLABII+ MEASURING CONSOLE

Stanisław Andrzej RÓŻAŃSKI

Stanisław Staszic University of Applied Sciences in Piła, Podchorążych 10, 64-920 Piła, Poland, srozansk@asta-net.com.pl

DOI: https://doi.org/10.24136/jaeee.2022.010

Abstract – The Coach6 software and the CoachLabII+ measuring console coupled with a computer and equipped with appropriate voltage and current sensors were used to determine the current-voltage and power-voltage characteristics of the photovoltaic cells. The current-voltage and power-voltage characteristics for a single cell and cells connected in series and in parallel were tested depending on the light intensity. Using a simplified theoretical model of a photovoltaic cell based on the one-diode equivalent circuit and Shockley diode equation, the ideality factor, diode saturation current and source current were determined, fitting the appropriate theoretical relationship to the measurement results. Based on the current-voltage and power-voltage characteristics, the short-circuit current, open circuit voltage, maximum power, fill factor, conversion efficiency and load resistance were determined. The dependence of the determined parameters on the light intensity was discussed.

Keywords – CoachLabII+ console, current-voltage characteristics, maximum power, one-diode model, photovoltaic cell

INTRODUCTION

The renewable energy sources are becoming in today's reality an important alternative to obtaining clean and emission-free energy necessary for the functioning of the economy and the advance of the prosperity of civilization [1, 2]. Particularly great interest and the development of new energy sources is related to photovoltaic panels (PV) that use a direct conversion of the photon's energy of the electromagnetic radiation into electricity [3, 4]. The photovoltaic effect, discovered by Becquerel in 1839, belongs to the group of internal photoelectric phenomena. Moreover, the solar energy is used to power residential buildings, cars, watches, calculators, etc. Thanks to systems based on PV cells, the security and energy independence of households is increasing, especially in the perspective of growing energy prices on the market.

The technology of PV cells is based mainly on the semiconductor properties of silicon and is constantly being improved. Semiconductor materials used in PV panels are either crystalline, polycrystalline or amorphous form. The production of crystalline silicon is based on a method developed by the Polish scientist Czochralski [5]. Other well-known semiconductor materials include germanium (Ge), copper oxide (Cu_2O), selenium, PbTe, PbS, SiC, InSb, GaAs and graphite. At absolute temperature an ideal semiconductor crystal would be an insulator. Characteristic semiconductor features are caused by thermal excitations, impurities, defects of crystal lattice and slight differences in chemical composition. Semiconductors, and mainly silicon are used to build diodes, transistors, integrated circuits or microprocessors [6].

However, the investigations are conducted on a large scale to increase the efficiency of PV cells by using other materials, e.g., dyes, perovskites, nanocomposite systems, liquid crystals, etc. [7-10].

In order to study the parameters affecting the efficiency of PV panels (e.g., ideality factor, series and shunt resistance), mathematical models are used to simulate the operation of PV in environmental conditions and their optimization [11]. In the simulation process, I-V and P-V characteristics are obtained and compared to the characteristics of the real PV panels. Various models are proposed to analyze the I-V characteristics of a PV cell [12-16]. One of the most popular solutions is based on the one-diode equivalent circuit and Shockley equation model [12]. In order to predict the power of the PV panel, simulations are carried out for standard conditions, i.e., temperature 298 K, light intensity 1000 W/m^2 and the solar spectrum AM 1.5 [13]. The efficient methods for determining the basic parameters of a PV cell from a single I-V characteristic using the Lambert W function were proposed [14, 15]. The determined equation for the current depends only on such parameters as ideality factor n, the series resistance R_s, and

the shunt resistance R_p [15]. Another method proposes to determine the basic parameters of a PV cell from the I-V characteristic consists in the combination of an improved constant illumination level method and the fitting method [16].

The paper presents a short review of photovoltaic cells based on various methods of converting photon energy into electric current and the use of a simplified theoretical description of the current-voltage characteristic to determine the basic parameters of photovoltaic cells.

I. TYPES OF SOLAR CELLS

Several generations of photovoltaic cells can be distinguished due to their construction and the materials used in which the process of photon energy conversion into electric current takes place [17]. The process of converting photon energy into electrical or chemical energy is a three-stage process involving the formation of an exciton (electron-hole pair), separation and migration of electrons and holes to the external circuit.

The first-generation photovoltaic cells can be made of crystalline or amorphous silicon. Monocrystalline silicon is produced by the Czochralski method already mentioned above [5]. The efficiency of monocrystalline cells is around 22%. Polycrystalline cells are obtained by melting silicon in special forms, grinding the surface and applying current paths by screen printing. The efficiency of this type of cells is 15-18% and they are more often used on the market.

In order to improve the PV cell efficiency, its upper surface is covered with an anti-reflective layer. The PV module consists of many interconnected PV cells that are secured to surface with EVA foil (Ethylene Vinyl Acetate foil), and on the bottom with PET foil (polyethylenterephthalat foil). The whole system is placed in a stiffened frame aluminum closed with tempered glass. The module contains the appropriate pins electric.

The second-generation PV cells are thin-film cells (layer thickness greater than or equal to 1 μm) usually made of amorphous silicon a-Si (efficiency 6-8%), cadmium telluride CdTe (efficiency 12-17%) or indium copper selenide CIGS (efficiency 13 -16%). They are made by sputtering a thin layer or many layers of a given material onto the surface of glass or metal. An interesting solution are HIT (Heterojunction with Intrinsic Thin layer) cells with an efficiency of 22.8%, built on the basis of a single layer of n-type monocrystalline silicon, adjacent to thin layers of n-type amorphous silicon on one side and p-type on the other side [18].

Another example in the construction of PV cells are silicon photovoltaic cells made with back electrode technology (Back Contact or Metal Wrap Through) achieving very high efficiency of over 22% [19]. Placing the electrode on the back of the cell saves the active surface of the top layer, which increases its efficiency.

The third-generation of PV cells is based on a reversible photochemical process in which a dye plays a major role (Dye-Sensitized Solar Cell – DSSC, DSC or DYS) [20]. It is a multi-layer structure consisting of a porous titanium oxide (TiO_2) semiconductor saturated with dye, an electrolyte consisting of a solution of iodine and potassium iodide, and a platinum catalyst layer. All components are sealed in a glass cell with appropriate TCO (Transparent Conducting Oxide) electrodes. The efficiency of DSSC cells is around 15%, and the advantage is the possibility of applying, for example, on the glass of building windows.

The PV cells operating on the principle of other physical phenomena include cells that use nano-structural materials. TiO_2 sensitized with quantum dots of cadmium selenide (CdSe) or cadmium sulfide (CdS) placed in an appropriate electrolyte can act as a layer that converts light energy into electricity [21]. The system is closed in a sealed glass cell with sputtered electrodes. By changing the size of quantum dots, they can be sensitized to specific wavelengths, similarly to cells with a dye. Quantum dots can also be dispersed in poly(methyl methacrylate) (PMMA) polymer matrix, where the light absorbed by them is transported to PV cells placed on the edges.

II. PEROVSKITE SOLAR CELLS

Perovskite photovoltaic cells are a promising class of new generation solar cells based on the properties of inorganic chemical compounds with the general structural formula ABX_3, where A is usually a cation from the alkali metals or alkaline earth metals group, B is a cation with a coordination number of 6 (usually titanium, niobium, tantalum, manganese) and X is typically the oxygen anion O^{2-}. The name of this group comes from the representative material which is perovskite (calcium titanate (IV), $CaTiO_3$). In recent years, the efficiency of perovskite cells has increased from 3.8% up to over 23.7%. In particular, lead-halide perovskites $(CH_3NH_3)_{0.80}(Cs)_{0.20}PbI_2Br$ have unique physicochemical properties such as appropriate conduction band gap, high extinction coefficient and long carrier lifetimes. This compound was used to form thin films using a one-step deposition method [22]. Moreover, solar cells based on mechanochemically prepared perovskite had efficiencies 10% higher than those with traditional solvent-based perovskite.

A perovskite cell usually consists of a conductive FTO (Fluorine Tin Oxide) substrate, an electron transport layer (ETL), a layer of perovskite and porous TiO_2, a hole transport layer (HTL) and an Au/Ag metal electrode. The perovskite layer illuminated by light absorbs photons and injects electrons into the conduction band of TiO_2, and the generated holes are transported to the hole-containing layer. The band gap of TiO_2 is about 1.5 eV.

Perovskite cells are characterized by greater mechanical resistance compared to silicon cells, which are relatively heavy, stiff and brittle. They can produce electricity even when it is cloudy or in the shade and with artificial lighting. They are also less sensitive to the setting in relation to the direction of the incident light. Perovskite cells can be produced at temperatures up to 373 K, while a temperature of around 1300 K is needed to melt silicon, which significantly reduces production costs. Interestingly, perovskite cells can be applied to any surface (e.g., car bodies, building facades, etc.) using painting or printing technology, thanks to which they are thin and flexible.

III. LIQUID CRYSTALS IN PHOTOVOLTAICS

As already mentioned in paragraph 1, organic materials are more and more often used in the construction of photovoltaic cells due to their easy availability and great possibilities of modifying their structure [9, 10, 23]. Liquid crystals are of great interest because of their self-organizing properties. Liquid crystals are a state of matter with an intermediate order between isotropic liquids and crystals. There are two main classes of liquid crystals, thermotropic and lyotropic. The molecules of thermotropic liquid crystals have either a calamitic or discotic molecular shape. Due to the arrangement of calamitic molecules, nematic, cholesteric and smectic mesophases are distinguished [24]. Liquid crystals can be successfully used to modify the properties and efficiency of PV dye cells as well as those based on perovskite technology [25].

Consider the operation of an organic PV cell on the example of using discotic liquid crystals [23, 26]. Discotic liquid crystals are columnar phases where the columns form conductive molecular wires due to the conductive aromatic core of the molecule. In contrast, the flexible tails on the edges of discotic molecules behave as an insulator. Columnar phases are characterized by a high degree of uniaxial charge-carrier mobility and show amazing ability to electron and hole conductivity. In the multi-layer structure of the PV device, discotic liquid crystal hexa-peri-hexabenzocoronene (HBC) is used in combination with perylene dye forming a large interfacial contact area [23]. The created junction structure in the form of a diode exhibits a fairly efficient photovoltaic effect. In addition, a method was presented to increase the power conversion efficiencies of solar cells by placing a layer of discotic liquid crystal hexabutyloxytriphenylene (HAT4) between the active layer and the hole transport layer [27]. HAT4 molecules placed in the active layer contribute to improving the mobility of charges.

An interesting application of liquid crystals is the modification of the electrolyte in DSSC cells [28]. The innovative electrolyte contains of two-component liquid crystal consisting of a carbonate-based mesogen and an ionic liquid, which self-assembles into a two-dimensional structure forming a well-defined conduction path for the ions. DSSC cells containing this electrolyte are characterized by exceptional open-circuit voltages and increasing power conversion efficiencies with increasing temperature.

IV. PHOTOVOLTAIC EFFECT

As already mentioned in the introduction, pure silicon at absolute zero temperature is an insulator. After increasing the temperature, the phenomenon of intrinsic conductivity associated with the breaking of the valence bonds in the silicon crystal lattice is observed. In practice, crystalline silicon is doped with atoms from the third group (by the old nomenclature) of the periodic table, e.g., indium (In), and p-type semiconductors (hole conductivity) with an excess of holes are obtained. The extra energy band that results from these extra holes at absolute zero lies slightly above the bottom of the valence band and is called the acceptor band.

However, doping silicon with atoms from the fifth group of the periodic table, e.g., arsenic (As), produces n-type semiconductors with electrons excess (electronic conductivity). In this case, the extra energy band that results from these extra electrons at absolute zero lies slightly below the bottom of the conduction band and is called the donor band.

After the formation of the p-n junction, an excess of high-energy electrons is contained in an n-type semiconductor, it passes through the contact surface to the p semiconductor and connects with excess of positive charges. At the same time, the holes move from p to n side and recombine with excess of electrons. This process continues until the Fermi levels are equals on both sides of the joint. This leads to the creation of a potential barrier at the junction, because the semiconductor n charges positively and p charges negatively. In the transition area, called the depletion area, an internal electric field is created.

When a p-n junction is illuminated with light, an electron-hole pair (exciton) is formed. In the internal electric field, the electrons are carried towards the semiconductor type n, and the holes in the direction of the p-type semiconductor. A potential difference arises between the electrodes of the cell equivalent to the voltage V_{OC} called the open circuit voltage. For a short circuit in a cell, a current flow through the cell with an short-circuit current I_{SC}, and its density j_{SC} is defined by the relationship:

$$j_{SC} = \frac{I_{SC}}{S}, \tag{1}$$

where S means the active surface of the PV cell.

The absorption of photons causes the electrons to move from the valence band to the conductivity band only when the photon energy E_f is greater than the energy gap width E_g, that is:

$$E_f = hf = \frac{hc}{\lambda} > E_g, \tag{2}$$

where Planck's constant h = $6{,}63 \cdot 10^{-34}$ Js, speed of light c = $3 \cdot 10^{8}$ m/s, f is the frequency of electromagnetic wave, and λ is the wavelength of light.

V. MODELLING OF SOLAR CELLS

A simplified schema of the equivalent circuit of the single diode model of PV cell is shown in Figure 1. The solar cell can be represented as a current source I_{ph} connected parallel with the diode. The diagram also takes into account two resistances R_s connected in series and R_p connected in parallel. R_s is related with the Joule effect losses due to the metal gride, semiconductors materials, etc. [11]. R_p is called the parallel leakage resistance or shunt resistance. Its typical value is greater than 100 kΩ and may be omitted in many applications, except for low lighting.

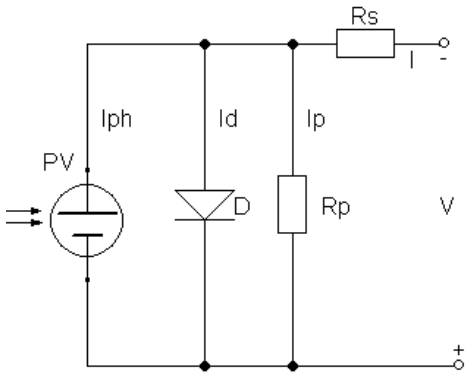

Fig. 1. Diagram of the equivalent circuit of PV cell

In this case, the output current I can be expressed by the following equation [12]:

$$I = I_{ph} - I_0\left[\exp\left(\frac{q(V+IR_s)}{nk_BT}\right)-1\right]-\frac{V+IR_s}{R_p}, \qquad (3)$$

where I_0 is a diode saturation current, q is an electron charge ($1.6\cdot10^{-19}$ C), k_B is a Boltzmann constant ($1.38\cdot10^{-23}$ J/K), n is an ideality factor (from 1 to 2), T is an absolute temperature. Since the value of R_p can be treated as infinite, equation (3) takes the form:

$$I = I_{ph} - I_0\left[\exp\left(\frac{q(V+IR_s)}{nk_BT}\right)-1\right]. \qquad (4)$$

In the case of ideal PV cell, the equation (4) simplifies to the form:

$$I = I_{ph} - I_0\left[\exp\left(\frac{qV}{nk_BT}\right)-1\right], \qquad (5)$$

where the second term in the equation (5) represents the known Shockley's diode current I_D formula for semiconductor materials.

It should be noted that the equation (3) cannot be solved analytically. However, with the help of Lambert W function, the solution can be given as [14, 15]:

$$I = \frac{V}{R_s} - \frac{R_p(R_sI_{ph}+R_sI_0+V)}{R_s(R_p+R_s)} + \frac{nk_BT}{qR_s}\text{lambertw} \times\left[\frac{qI_0R_pR_s}{nk_BT(R_p+R_s)}\exp\left(\frac{R_pq(R_sI_{ph}+R_sI_0+V)}{nk_BT(R_p+R_s)}\right)\right], \qquad (6)$$

where lambertw means Lambert W function. The parameters I_0, I_{ph}, n, R_s, R_p can be obtained using numerical fitting method of the photovoltaic cell I-V characteristics found experimentally.

VI. CURRENT-VOLTAGE CHARACTERISTICS OF A SOLAR CELL

For an ideal PV cell, the current-voltage characteristics I- V should have rectangular shape with sides I_{SC} and V_{OC}. Maximum power of an ideal cell $P_i = I_{SC}V_{OC}$ is always greater than the maximum power of the real cell $P_{max} = I_mV_m$, where I_m and V_m are the coordinates of the point P located at the maximum power (Figure 2). The blue line in Figure 2 shows the power-voltage (P-V) characteristics of the PV cell with the marked maximum power point.

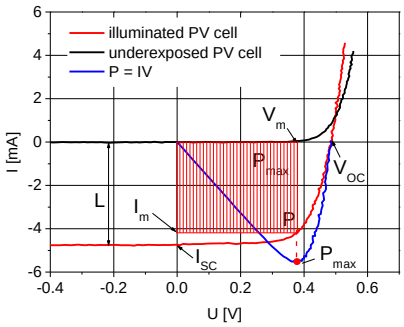

Fig. 2. The basic parameters describing the current-voltage characteristics of the PV cell

The conversion efficiency η of a PV cell is defined as the ratio of the maximum power P_{max} real cell to the power of radiation incident on the cell:

$$\eta = \frac{P_{max}}{LS}, \qquad (7)$$

where L is the intensity of radiation incident on the cell and S is the PV cell area.

The parameter called the fill factor (FF) can be determined from the formula:

$$FF = \frac{P_{max}}{I_{SC}V_{OC}}, \qquad (8)$$

which after substituting to (7) gives the equation on the nominal conversion efficiency of a PV cell:

$$\eta = \frac{I_{SC}V_{OC}FF}{LS}. \qquad (9)$$

The optimal PV cell load resistance is:

$$R = \frac{V_m}{I_m}. \qquad (10)$$

VII. MEASUREMENTS

To determine the I-V characteristics of a photovoltaic cells, the CMA (Centrum voor Microcomputer Applicaties) measurement system was used, which enables acquisition data and automation of physical measurements. The system includes the CoachLabII+ console, sensors of various physical quantities (e.g., temperature, pressure, force, light intensity, current, voltage) and the Coach6 software enabling the analysis of the data, and, more importantly, modeling and performing simulation [29]. CoachLabII+ has its own microprocessor, flash memory, external power supply, and is connected to the computer via a USB port. Figure 3 shows a picture of the CoachLabII+ console and the following elements:

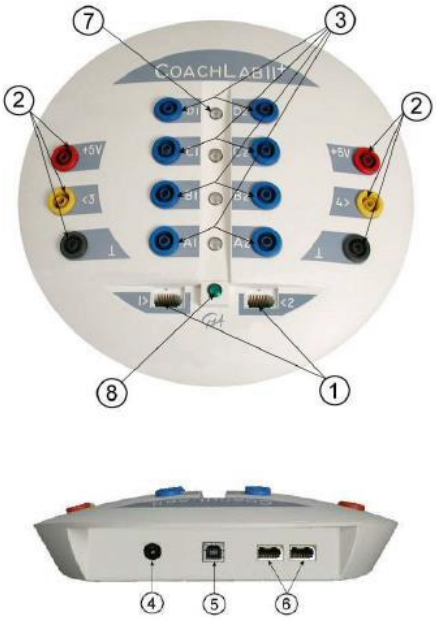

Fig. 3. The view of the CMA CoachLabII+ console [6]

- two analog BT (British Telecom) type inputs (1),
- two 4mm analog inputs (2),
- four pairs of bidirectional outputs (3),
- connecting the external power plug (4),
- connecting the USB cable (5),
- two digital inputs for connecting ultrasonic sensors (6),
- four LEDs indicating the status of each digital channel (7),
- green LED indicating that the interface is properly powered (8).

Figure 4 shows graphical interface of the Coach6 software that enables to control the course of the experiment, change of the experiment parameters and data collection. The results are presented in the graphic, table and analog meters form. Moreover, Figure 2 shows an example of the recorded current-voltage characteristics of a single

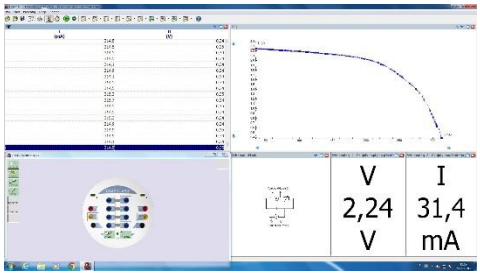

Fig. 4. Graphical panel of the Coach6 software

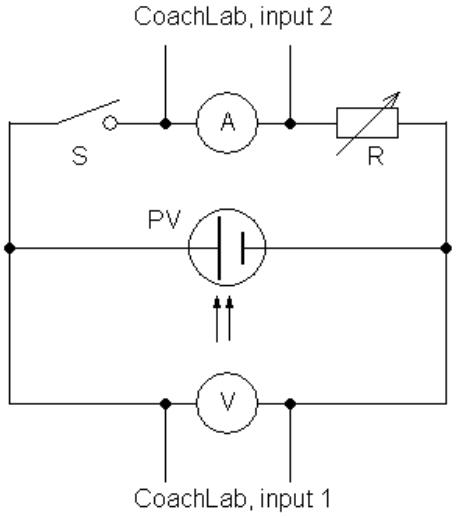

Fig. 5. Scheme of measurement setup: A – ammeter, V – voltmeter, PV – photovoltaic cell, R – potentiometer, S – switch

photovoltaic cell for the chosen light intensity.

Two photovoltaic panels with an area of $S = 8.25 \cdot 10^{-3}$ m^2 each were used in the experiment. The panels were connected in series and in parallel. The measurements were dan in the temperature of about 300 K. An incandescent lamp was used to illuminate the PV panels.

The CMA 0222i current sensor with a measuring range from -500 mA to +500 mA and the CMA 0210i differential voltage sensor with a range of -10 V to +10 V were used. The light intensity was measured with the data logger light meter AB-8809A. The measuring system also uses a variable resistor module with a range of 100 Ω. The connection diagram of the measuring system elements is shown in the Figure 5.

VIII. RESULTS AND DISCUSSION

Figure 6 shows the current-voltage (I-V) characteristics of the solar cell for different light intensities. For small voltages, the relationship I(V) is linear and nearly parallel to the V axis for all intensities. With increasing the voltage, the dependence stays systematically more nonlinear and for V_{oc} decreasing to zero. With decreasing light intensity, the I-V characteristic shifts to the lower values of current. The short-circuit current I_{SC} decreases with decreasing illuminance as well as the slight decrease of V_{OC} voltage is observed. The solid lines shown in Figure 6 were obtained by fitting the measurement results with the equation (5). Despite many simplifications in the formula (5), a fairly good fitting of the data was obtained.

The obtained fitting parameters from equation (5) are collected in Table 1.

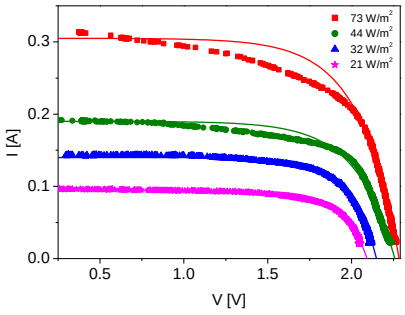

Fig. 6. The I-V characteristics of the PV cell for different light intensities

Table 1. Fitting parameters obtained from equation (5)

L [W/m²]	73	44	32	21
I_{ph} [A]	0.30	0.19	0.14	0.09
I_0 [A]	$1.7 \cdot 10^{-5}$	$9.5 \cdot 10^{-6}$	$1.1 \cdot 10^{-7}$	$3 \cdot 10^{-8}$
n	9.0	8.8	5.9	5.4

The values of the I_{th} presented in Table 1 are consistent with the I_{SC} values read from the I-V characteristics. Furthermore, the high values of the recombination current ideality factor much greater than 2 require some discussion. The Shockley-Read-Hall recombination theory predicts that the value of n should be equal to or less than 2 [30]. However, the one explanation of this problem is to take into account that such a recombination current does not flow uniformly through the cell, but always at local sites, e.g., in extended defects [30].

Figure 7 shows the power-voltage dependence for the different light intensities. With decreasing intensity, the maximum power point decreases and shifts to the slightly lower voltage values. The read values of I_{sc}, U_{OC}, P_{max} from the graphs presented in Figures 6 and 7, and the R, FF, η values calculated on the basis of the formulas presented in paragraph 6 are shown in Table 2.

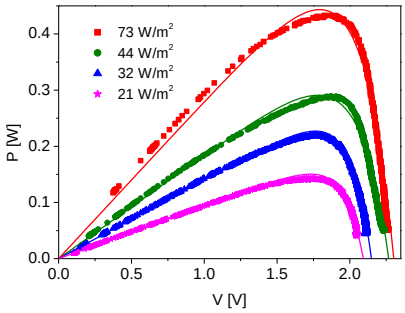

Fig. 7. The P-V characteristics of the PV cell for different light intensities

Table 2. Parameters of the solar cell used in experiment

L [W/m²]	73	44	32	21
I_{SC} [A]	0.31	0.19	0.14	0.09
V_{OC} [V]	2.27	2.24	2.12	2.06
P_i [W]	0.70	0.43	0.30	0.19
I_m [A]	0.23	0.16	0.12	0.08
V_m [V]	1.86	1.86	1.78	1.72
P_{max} [W]	0.43	0.29	0.22	0.14
R [Ω]	8.10	11.63	14.83	21.50
FF	0.62	0.68	0.74	0.77
η	0.72	0.80	0.83	0.82

The values of the FF and η parameters of investigated solar cell presented in Table 2 slightly increase with the decrease in the light intensity. The observed effect of light intensity on the solar cell parameters is consistent with theoretical predictions and the results of the other experiments [31].

Table 3. Parameters of the solar cells connected in series and in parallel for different light intensities

	parallel		series	
L [W/m²]	44	32	44	32
I_{SC} [A]	0.25	0.17	0.14	0.10
V_{OC} [V]	2.11	2.13	4.07	4.19
P_i [W]	0.53	0.36	0.57	0.42
I_m [A]	0.23	0.16	0.17	0.09
V_m [V]	1.64	1.80	3.43	3.73
P_{max} [W]	0.38	0.29	0.40	0.35
R [Ω]	7.13	11.25	20.18	37.44
FF	0.72	0.81	0.70	0.83
η	0.53	0.55	0.55	0.66

Figure 8 shows I-V characteristics of solar cells connected in series and in parallel for different light intensities. For the solar cells connected in parallel the I_{SC} current increases but V_{OC} voltage proportionally decreases in comparison with the cell system connected in series.

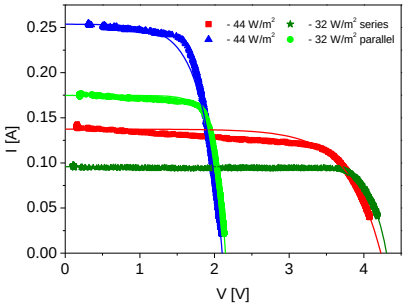

Fig. 8. The I-V characteristics for solar cells connected in series and in parallel for different light intensities

Figure 9 shows the power-voltage characteristics of solar cells connected in series and in parallel for chosen light intensities. The power maxima of the P-V characteristics for

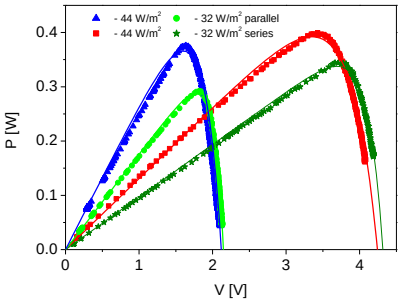

Fig. 9. The P-V characteristics for solar cells connected in series and parallel for different light intensities

the solar cells connected in parallel are shifted to the higher voltage values compare to the in series connections. Moreover, if the light intensity decreases the power maxima are also decreasing and shifts to the higher voltages for a given intensity. The appropriate parameters derived from the I-V and P-V characteristics are presented in Table 3. The solid lines presented on the Figure 8 and 9 were obtained by fitting I-V and P-V characteristics with equation (5). The obtained fitting parameters are collected in Table 4.

Table 4. Fitting parameters for the solar cells connected in series and in parallel for different light intensities

	parallel		series	
L [W/m²]	44	32	44	32
I_{th} [A]	0.137	0.096	0.175	0.258
I_0 [A]	$8.23 \cdot 10^{-6}$	$2.06 \cdot 10^{-10}$	$8.13 \cdot 10^{-8}$	$14 \cdot 10^{-5}$
n	16.79	8.32	5.69	10.90

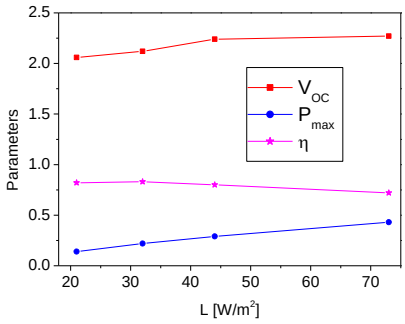

Fig. 10. Parameters of the I-V characteristics for solar cell at different light intensities

Figure 10 shows light intensity dependence of some parameters presented in Table 2. Although the measurements were made only for a few light intensities, a tendency to saturation or decrease of these parameters can be observed with increasing intensity.

IX. CONCLUSIONS

Using the CoachLabII+ console, appropriate sensors and dedicated Coach6 software, measurements of the I-V and P-V characteristics of the photovoltaic panels connected in series and in parallel were performed. The obtained results were analyzed using the one-diode equivalent circuit and Shockley equation model. The parameters such as n, I_{th}, I_0 obtained from the fits have quite realistic values. However, they are burdened with a rather significant uncertainty resulting from the simplified theoretical formulas and measurement uncertainties. The basic parameters of the panels were read from the I-V and P-V characteristics for a given light intensity. The observed regularities are consistent with the studies of this type of systems compared to the literature. The usefulness of the CoachLabII+ measurement console in a student physics laboratory has been demonstrated, where the described system can be used to better understand the physical phenomena accompanying the photovoltaic effect. The applied system acquaints students with the measurement methods used in professional scientific laboratories, where the automation of physical measurements and data processing are often used.

WYZNACZANIE CHARAKTERYSTYK PRĄDOWO-NAPIĘCIOWYCH OGNIW FOTOWOLTAICZNYCH Z WYKORZYSTANIEM KONSOLI POMIAROWEJ COACHLABII+

Do wyznaczenia charakterystyk prądowo-napięciowych oraz mocowo-napięciowych ogniw fotowoltaicznych wykorzystano oprogramowanie Coach6 oraz konsolę pomiarową CoachLabII+ sprzężoną z komputerem i wyposażoną w odpowiednie czujniki napięcia i prądu. Charakterystyki prądowo-napięciowe dla pojedynczego ogniwa oraz ogniw połączonych szeregowo i równolegle badano w zależności od natężenia światła. Wykorzystując uproszczony model teoretyczny ogniwa

fotowoltaicznego bazujący na pojedynczej diodzie oraz wzorze Shockley'a dla prądu diody półprzewodnikowej wyznaczono współczynnik korekcji, prąd wsteczny oraz prąd źródła, dopasowując odpowiednie zależności teoretyczne do wyników pomiarów. Na podstawie charakterystyk prądowo-napięciowych oraz mocowo-napięciowych wyznaczono prąd zwarcia, napięcie obwodu otwartego, moc maksymalną, współczynnik wypełnienia, sprawność konwersji ogniwa oraz rezystancję obciążenia. Zaobserwowano zależność wyznaczonych parametrów od natężenia światła.

Słowa kluczowe: charakterystyka prądowo-napięciowa, konsola CoachLabII+, moc maksymalna, model jednodiodowy, ogniwo PV

REFERENCES

[1] Owusu P.A., Asumadu-Sarkodie S. (2016) "A review of renewable energy sources, sustainability issues and climate change mitigation". Cogent Engineering. Vol. 3, 1167990, doi: 10.1080/23311916.2016.1167990

[2] Ellabban O., Abu-Rub H., Blaabjerg F. (2014) "Renewable energy resources: Current status, future prospects and their enabling technology". Renewable and Sustainable Energy Reviews. Vol. 39, pp 748-764, doi: 10.1016/j.rser.2014.07.113

[3] Fouad M.A., Shihata L.A., Morgana El-S.I. (2017) "An integrated review of factors influencing the perfomance of photovoltaic panels". Renewable and Sustainable Energy Reviews. Vol. 80, pp 1499-1511, doi: 10.1016/j.rser.2017.05.141

[4] Muteri V., Cellura M., Curto D., Franzitta V., Longo S., et al. (2020) "Review on life cycle assessment of solar photovoltaic panels". Energies. Vol. 13, 252, doi: 10.3390/en13010252

[5] Tomaszewski P.E. (2002) "Jan Czochralski—father of the Czochralski method". Journal of Crystal Growth. Vol. 236, Issues 1–3, pp 1-4, doi: 10.1016/S0022-0248(01)02195-9

[6] Sze S.M., Li Y., Ng K.K. "Physics of Semiconductor Devices". John Wiley & Sons 2021.

[7] Kaur N., Singh M., Pathak D., Wagner T., Nunzid J.M. (2014) "Organic materials for photovoltaic applications: Review and mechanism". Synthetic Metals. Vol. 190, pp 20-26, doi: 10.1016/j.synthmet.2014.01.022

[8] Snaith, H.J. (2018) "Present status and future prospects of perovskite photovoltaics". Nature Mater 17, pp 372–376, doi: 10.1038/s41563-018-0071-z

[9] Martínez-Miranda L.J. (2022) "Liquid crystals in photovoltaics". CRC Press, Boca Raton, Taylor & Francis Group. doi: org/10.1201/9781351175784

[10] Kumar M., Kumar S. (2017) "Liquid crystals in photovoltaics: A new generation of organic photovoltaics". Polymer Journal. Vol. 49, pp 85–111, doi: org/10.1038/pj.2016.109

[11] Vinod, Kumar R., Singh S.K. (2018) "Solar photovoltaic modeling and simulation: As a renewable energy solution". Energy Reports. Vol. 4, pp 701–712, doi: 10.1016/j.egyr.2018.09.008

[12] Tamrakar V., Gupta S.C., Yashwant S. (2015) "Single-diode PV cell modeling and study of characteristics of single and two-diode equivalent circuit". Electrical and Electronics Engineering: An International Journal. Vol 4, pp 13-24 doi: 10.14810/elelij.2015.4302

[13] El-Ahmar M.H., El-Sayed A.-H.M., Hemeida A.M., (2016) "Mathematical modeling of photovoltaic module and evalute the effect of varoius paramenters on its performance". Eighteenth International Middle East Power Systems Conference (MEPCON), pp 741-746, doi: 10.1109/MEPCON.2016.7836976

[14] Peng L., Sun Y., Meng Z., Wang Y., Xu Y. (2013) "A new method for determining the characteristics of solar cells". Journal of Power Sources. Vol. 227, pp 131-136, doi: 10.1016/j.jpowsour.2012.07.061

[15] Zhang Ch., Zhang J., Hao Y. Lin Z., Zhu Ch. (2011) "A simple and efficient solar cell parameter extraction method from a single current-voltage curve". Journal of Applied Physics. Vol. 110, 064504, doi: 10.1063/1.3632971

[16] Ishibashi K., Kimura Y., Niwano M. (2008) "An extensively valid and stable method for derivation of all parameters of a solar cell from a single current-voltage characteristic". Journal of Applied Physics. Vol. 103, 094507, doi: 10.1063/1.2895396

[17] Pastuszak J., Węgierek P. (2022) "Photovoltaic cell generations and current research directions for their development". Materials. Vol. 15, 5542, doi: 10.3390/ma15165542

[18] De Wolf S., Descoeudres A., Holman Z.C., Ballif Ch. (2012) "High-efficiency Silicon Heterojunction Solar Cells: A Review". Green. Vol. 2, pp. 7–24, doi: 10.1515/green-2011-0018

[19] Wu Y., Van Aken B.B., Janssen G., J. Loffler J., Li F., et al. (2014) "Metal wrap through silicon heterojunction solar cells and first made minimodules". Conference EuPVSEC 2014, Amsterdam

[20] Sharma K., Sharma V., Sharma S.S. (2018) "Dye-sensitized solar cells: Fundamentals and current status". Nanoscale Research Letters. Vol. 13:381, doi: 10.1186/s11671-018-2760-6

[21] Abolghasemi R., Rasuli R., Alizadeh M. (2020) "Microwave-assisted growth of high-quality CdSe quantum dots and its application as a sensitizer in photovoltaic cells". Materials Today Communications. Vol. 22, 100827, doi: 10.1016/j.mtcomm.2019.100827

[22] Zuo Ch., Bolink H.J., Han H., Huang J., Cahen D., Ding L. (2016) "Advances in perovskite solar cells". Advances Science. Vol. 3, 1500324, doi: 10.1002/advs.201500324

[23] Schmidt-Mende L., Fechtenkotter A., Mullen K., Moons E. (2001) "Self-organized discotic liquid crystals for high-efficiency organic photovoltaics". Science. Vol. 293, pp. 1119-1122, doi: 10.1126/science.293.5532.1119

[24] Andrienko D. (2018) "Introduction to liquid crystals". Journal of Molecular Liquids. Vol. 267, pp 520–541, doi: 10.1016/j.molliq.2018.01.175

[25] Łempicka-Mirek K., Król M., Sigurdsson H., Wincukiewicz A., Morawiak P., et al. (2022) "Electrically tunable Berry curvature and strong light-matter coupling in liquid crystal microcavities with 2D perovskite". Science Advances. Vol. 8, eabq7533, doi: 10.1126/sciadv.abq753

[26] Bajpai M., Yadav N., Kumar S., Srivastava R., Dhar R. (2015) "Bulk heterojunction solar cells based on self-assembling disc-shaped liquid crystalline material". Liquid Crystals, Vol. 43, pp 305-313, doi: 10.1080/02678292.2015.1108466

[27] Zheng O., Guojia Fang G., Bai W., Sun N., Qin P., et al. (2011) "Efficiency improvement in organic solar cells by inserting a discotic liquid crystal". Solar Energy Materials & Solar Cells. Vol. 95, pp 2200–2205, doi: 10.1016/j.solmat.2011.03.024

[28] Högberg D., Soberats B., Uchida S., Yoshio M., Lars Kloo L., et al. (2014) "Nanostructured two-component liquid-crystalline electrolytes for high-temperature dye-sensitized solar cells". Chemical Materials. Vol. 26, pp 6496–6502, doi: 10.1021/cm503090z

[29] Różański S.A. (2020) "Computer-aided experiments in student physics laboratory". Acta Physica Polonica B Proceedings Supplement. Vol. 13, Issue 4. pp 937-942, doi: 10.5506/APhysPolBSupp.13.937

[30] Breitenstein O. (2013) "Understanding the current-voltage characteristics of industrial crystalline silicon solar cells by considering inhomogeneous current distributions". Opto–Electronics Review. Vol. 21, Issue 3. pp 259–282, doi: 10.2478/s11772-013-0095-5

[31] Chegaar M., Hamzaoui A., Namoda A., Petit P., Aillerie M., Herguth A. (2013) "Effect of illumination intensity on solar cells parameters". Energy Procedia. Vol. 36, pp 722 – 729, doi: 10.1016/j.egypro.2013.07.084